Journal of Metals, Materials and Minerals, Vol. 31, No. 3, pp. 118-126, 2021

Effect of DC power on the thickness, hardness and adhesion strength of Ti-51 at% Ni coated Ti/TiN

Ishiaka Shaibu ARUDI[1], Esah HAMZAH[1,*], Muhammad Azizi MAT YAJID[1], and Bushroa ABDUL RAZAK[2]

[1] *School of Mechanical Engineering, Faculty of Engineering, Universiti Teknologi Malaysia, 81310 UTM Johor Bahru, Johor Bahru, Malaysia*
[2] *Department of Mechanical Engineering, Faculty of Engineering, University of Malaya, 50603 Kuala Lumpur, Malaysia*

***Corresponding author e-mail:** esah@mail.fkm.utm.my

Received date:
5 February 2021
Revised date
13 September 2021
Accepted date:
17 September 2021

Keywords:
Characterisation;
Sputtering;
Thickness;
Hardness;
Adhesion

Abstract

The coating of Ti/TiN was successfully deposited on Ti-51 at% Ni substrates by using direct current (DC) magnetron sputtering technique and the effect of different sputtering power on the thickness, surface hardness and adhesion strength of the coatings were studied. The microstructural characterization was carried out using scanning electron microscope (SEM), energy-dispersive X-ray (EDX) and X-ray diffractometer (XRD). The coating thicknesses were detected and measured using SEM. The surface hardness test was performed using microhardness tester, and the adhesion strength was carried out by scratch testing. The results showed that the TiN crystallites growth orientation, thickness, surface hardness and adhesion strength are influenced by sputtering power. As power increased from 300 W to 370 W, peaks at (111), (200) and (311) increased while peaks at (200) and (222) decreased, substrate hardness increased by 53.42%, thickness increased from 2.278 μm to 2.389 μm, and adhesion strength also increased from 3000 mN to 3998 mN. Meanwhile, a decrease in thickness, hardness, adhesion strength, all the peaks and total disappearance of peak (222) were all noticed at 440 W.

1. Introduction

The use of near-equiatomic TiNi alloys, with nickel composition from 48% to 51% as biomaterials for implants is extensive because of their outstanding mechanical properties, high corrosion resistance, biocompatibility and their ability to exhibit shape recovery behaviour known as shape memory effect and superelasticity [1,2]. Additionally, Ti-Ni's ability to recover a substantial amount of strain (8%) when heated to body temperature is one of the mechanical properties that are almost like that of natural biomaterials, such as bone [3,4]. However, Ti-Ni shape memory alloys were restricted in the broader medical applications [5], despite their use as a biomaterial for a long time, this is because many research reports about Ni have shown that it can cause hypersensitivity to the human body due to its toxicity and allergenicity [6]. Many researchers have equally expressed concerns about the release of Ni ions from the Ti-Ni alloy's surface [7]. The toxic effect of high Ni concentrations in Ti-Ni alloys on soft tissues' structure will harm bone structures [8]. To overcome these factors limiting the application of Ti-Ni in bio-implants, different surface modification of Ti-Ni such as Physical Vapour Deposition (PVD), Ion Implantation, Chemical Vapour Deposition (CVD), Nitriding and Plasma Spray coating, are widely used [9-15]. In the list of coating methods, PVD magnetron sputtering technique proved to be more encouraging because of its low processing temperature which is typically in the range of 200°C to 400°C [16] on various coating thickness ranging between 0.5 μm and 3.0 μm [17-19]. The coating features of PVD magnetron sputtering can be regulated by controlling deposition parameters, such as temperature, input power, gas flow rate and substrate bias voltage [20].

Ti-N coating falls into bio-active coatings, enhancing both biological and mechano-chemical behaviours of Ti-Ni in its applications to the body [21]. Moreover, some of Ti-N properties, such as wear, and corrosion resistance are substantially higher than some bio-compatible compounds such as titanium carbide and titanium oxide [22,23]. Therefore, TiN is a bioactive coating that can minimise Ni ions' release from Ti-Ni surface and improve its corrosion resistance [24].

This work focuses on the effect of different deposition power on the thickness, surface hardness, and adhesion strength of Ti-51 at% Ni coated with TiN using the DC magnetron sputtering methods.

2. Experimental

2.1 Sample preparation

The substrate material used for the research was Ti-51 at% Ni supplied by Stanford Advanced Materials, USA and received as a product of a casting process in the form of a plate. The as-received Ti-51 at% Ni was cut into 15 mm × 15 mm length and 3 mm thickness by Electric Discharge Machining (EDM) wire cut for materials characterisation and a PVD coating. Samples for materials characterisation were prepared following standard sample preparation methods, including grinding on silicon carbide papers from grit no 220 to 1000 followed by polishing

on a polishing cloth with colloidal silica suspension. When a mirror-like surface was obtained, the sample was subjected to etching for 30 s to 45 s in an etching solution (HF:10, HNO3:40, H2O:50).

The Sample for magnetron sputtering coating was prepared following the same procedure used in the sample preparation for Optical Microscopy (OM), and Scanning Electron Microscopy (SEM)/ EDX exclusion of etching process carried out in the sample preparation for optical microscopy.

The substrate's initial surface to be coated was conducted by using surface roughness tester "SJ-310 Mitutoyo, Japan" to make sure that the surface roughness (Ra) before the coating was lower than 0.1 μm, this is to allow for better adhesion and less friction [25]. Before coating, the already prepared sample was further cleaned ultrasonically in acetone, alcohol, distilled water and then dried afterwards before being placed on the substrate holder of the magnetron sputtering system (TF450 Sputtering System, SG Control Engineering, Singapore). This cleaning process was carried out to eliminate contaminants from the substrate surface, increase the surface reactivity that is likely to occur and allow strong chemical bonds to form. Some of the substrates were partially covered using tape for thickness measurement.

2.2 Coating Process

The Coating of TiN substrate on Ti-51 at% Ni alloy with the aid of the DC magnetron sputtering system was carried out at the Surface Engineering Laboratory, University of Malaya, Kuala Lumpur. The system has a vertical setup with dual switchable services of DC and RF targets having 12 cm above the substrate holder. In these experiments, Ti disc of 101.6 mm diameter with a purity level of 99.99% and the 3 mm thickness was used as a target. The process of deposition was started by vacuuming the chamber down to a base pressure of 2.85×10^{-5} Torr. Afterwards, argon gas was purged into the chamber to form the plasma used on the target's surface to etch the native oxide layer. To remove any remaining surface contamination, the substrates were bombarded with ions in an argon flow discharge for 15 min at a negative bias voltage of -75 V. The substrates were then heated gradually to the required temperature of 200°C. The deposition of TiN which was performed in a mixed N_2-Ar atmosphere at ratio 1 : 5 was done by sputtering the Ti target coupled to DC power supply. The substrates were removed when the chamber's temperature was at room temperature and then taken for subsequent characterization. Table 1 summarizes the experimental conditions for producing TiN-layers. Under these conditions, the creation of stoichiometric gold-coloured TiN coating was possible, hard and dense coating was achieved.

2.3 Materials Characterization of coated and uncoated Ti 51 at% Ni

The Ti-51 at% Ni microstructure was examined with the aid of an OM, Olympus BX60. SJ-310 Mitutoyo. SEM/EDX was used to detect the uncoated sample surface morphology and elemental composition the coated sample's cross-sectional morphology to determine the coating thickness. EDX analysis in area scan mode was also used to determine the elemental distributions of Ti, Ni, N, and O. The profiles of the elements were determined across the layers from the bulk to the surface of the coating. X-Ray Diffraction (XRD) study was carried out to determine the phases and the crystalline structure of the coated Ti 51 at% Ni sample. The study was carried out by utilizing Rigaku Smart Lab X- Diffraction equipment with a 40 kV tube voltage and a 30 mA tube current using a monochromatic X-ray source of CuKα1 (α = 1.5406 Å) radiation. The range of scanning angle 2θ was between 30° and 90° with a step of 0.10°. The diffraction pattern obtained was reported on the graph as peaks.

Table 1. Sputtering parameters for TiN deposition.

Parameter				
Power (W)	**Temperature (°C)**	**Bias (V)**	**Pressure (mTorr)**	**Time (min)**
300	200	75	5	240
370	200	75	5	240
440	200	75	5	240

2.4 Hardness test

The hardness test for the coated and uncoated sample was conducted in a Microhardness tester (SHIMADZU Micro Hardness Tester, HMV-2 Series) at the Surface Engineering Laboratory, University of Malaya, Kuala Lumpur. The specimen to be examined was mounted on an anvil with a base of screw thread. The test was conducted by applying a controlled force of 1.9 N for 5 s with a square-based diamond pyramid indenter whose opposite sides converge at an angle of 1360 at the apex. The resulting indentation diagonal was determined under a microscope. The above steps were repeated three times at different locations on the coated and uncoated specimens, and the average vickers hardness value was recorded. For verification purposes, the measurement and the test load were used to manually calculate the vickers hardness value in a particular formula, as shown in formula (1).

$$HV = 0.1891 * F / d^2 \quad (1)$$

Where d is the average of the two imprint diagonals, and F is the load applied

2.5 Scratch adhesion test

The scratch adhesion test assesses the integrity and mechanical reliability of coated surfaces. The adhesion strength between substrate and coating is measured by employing the scratch test, also known as a quantitative technique. It is defined as total coating failure and commonly referred to as critical load (Lc). In this work, a scratch test machine manufactured by Micro Material Ltd. (Micro Material Nano test, Wrexham, UK) using a 25 μm sphero conical diamond indenter and 900 as an indenter was used to measure the adhesion strength of the TiN coated on the Ti-51 at% Ni. The test mode was a horizontal scratch with a single pass. In the test, a load of 4000 mN with a scanning length of 1000 μm and a loading rate of 3 $mN \cdot s^{-1}$ was applied on the coating, the coating failure was confirmed by comparing a depth graph versus distance with a scratch micrograph obtained using an optical microscope (Olympus BX 61). The coating failure was determined by matching the critical load (Lc2) in the micrograph to the onset of

coating failure. Lc2 indicates the adhesive failure point and indicates the strength of the interfacial adhesion in this coating/substrate system and is known as scratch adhesion strength [26].

3. Results and discussions

3.1 Characterization of uncoated and coated Ti-51 at% Ni

The results of characterization of the microstructure, indicated that the optical micrograph of the uncoated sample and its grain size distribution shown in Figures 1(a) and (b) respectively, is equiaxed having precipitate along the grain boundaries with an average grain size of 219 ± 65.2 μm calculated from ImageJ software. The FESEM microstructure shows the morphology of grain boundary precipitation and EDX spectrum indicated that the uncoated Ti-51 at% Ni consist mainly of Ti and Ni elements, as shown in Figures 2(a) and 2(b), which are homogenously distributed as illustrated in the mapping shown in Figures 2(c) and 2(b). Cross-sectional views of Ti/TiN coating at different DC powers shown in Figures 3(a, b and c), exhibit dense structures without any visible cracks or voids between the substrates and the coatings. The FESEM cross-sectional measurement showed that the different coating condition produced a different thickness. The EDX cross-sectional element line scan, which starts at the substrate and ends at the top layer shows N, O, Ti and Ni as

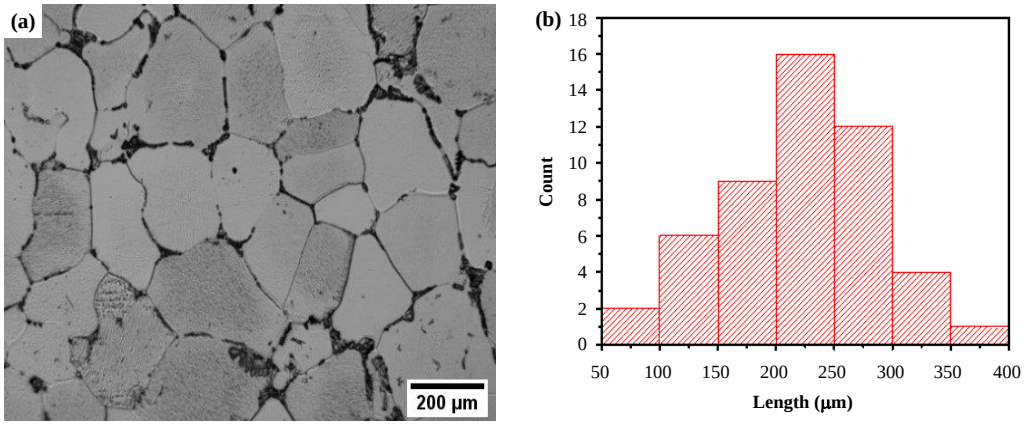

Figure 1. (a) Optical micrographs, and (b) grain size distribution of uncoated Ti-51 at% Ni.

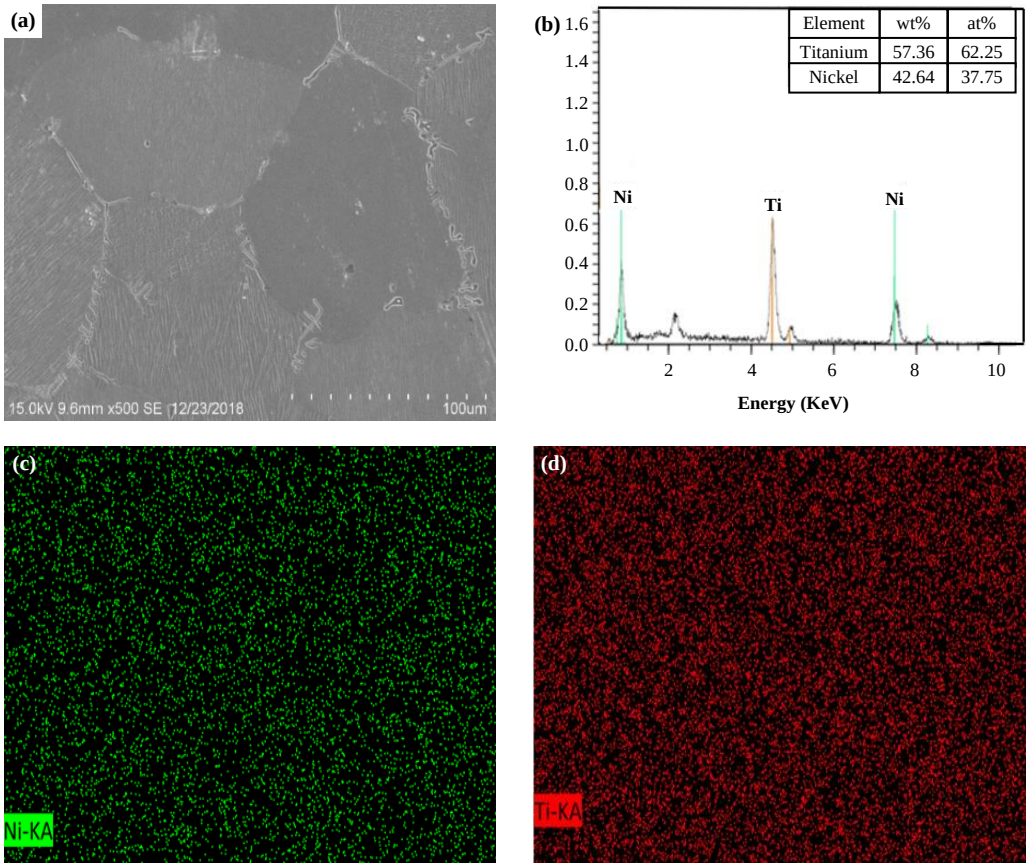

Figure 2. (a) SEM image of uncoated Ti-51 at% Ni, (b) EDX, mapping and (c) Ni (d) Ti.

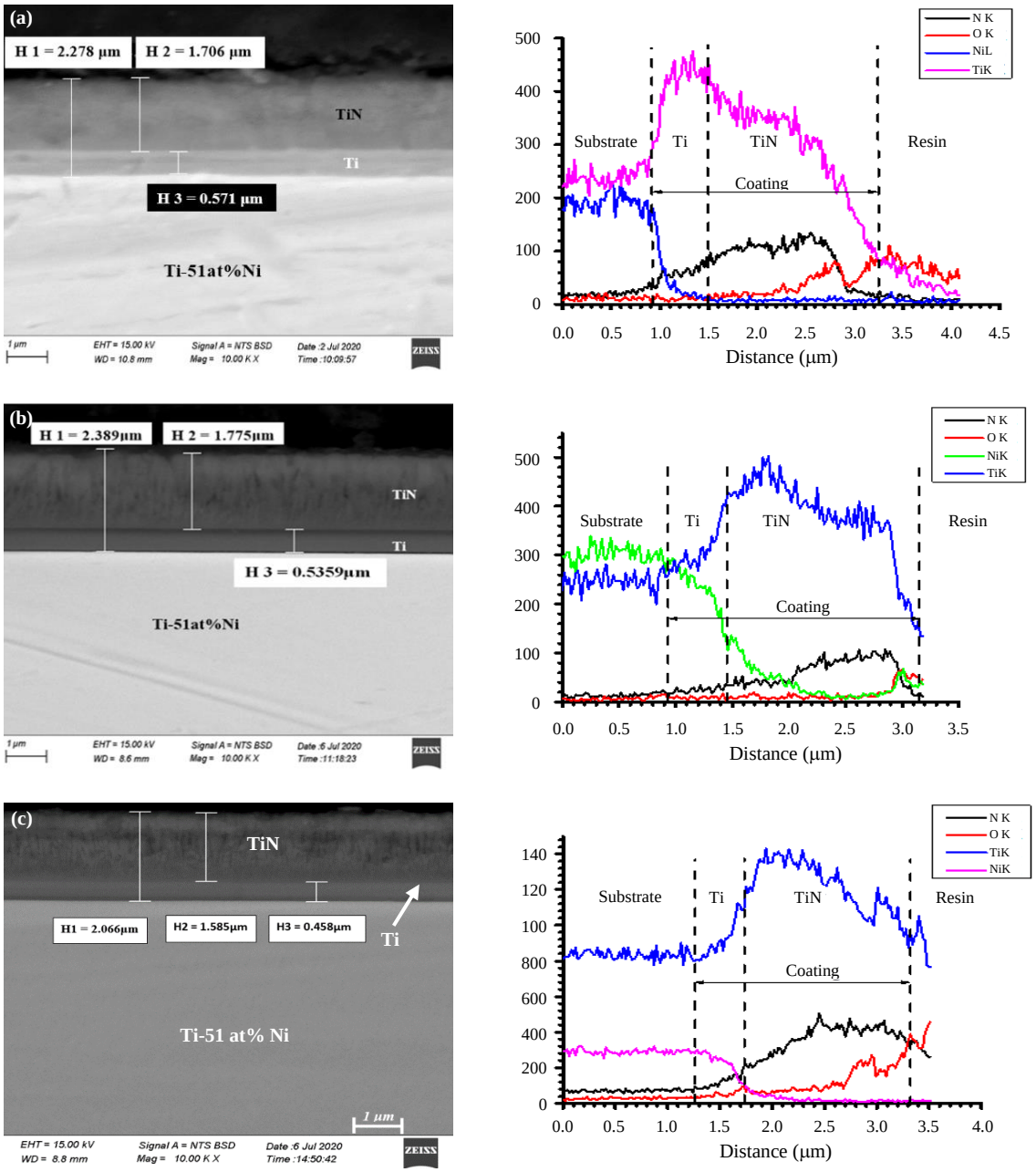

Figure 3. Cross-sectional FESEM images and line scanning of Ti/TiN coating with different DC power: (a) 300 W, (b) 370 W, and (c) 440 W.

the elements observed during the scanning process. The diffusion rate of all the elements are illustrated in Figure 3. The coating zone which is sub divided into Ti and TiN shows the behaviours of the line profiles of all the elements. The scanning showed that oxygen (O) and nitrogen (N) were present and their concentration increased gradually from the substrate to the final TiN layer. The Ti interlayer is very soft; it requires the mixing of nitrogen to enhance the interlayer's strength and hardness [27]. As the level of nitrogen doping increases, there is a general trend that the Ti interlayer's hardness increases, which is clearly due to the dissolution of nitrogen in the α-Ti lattice, that causes the solid solution to harden in the interlayer [28]. The improvement obtained in adhesion strength can be attributed to the increased strength of Ti interlayer-influenced nitrogen. As the Ti interlayer's acquired oxygen decomposes the native oxide film on the substrate's surface, the coating and substrate's adhesion are also improved. The Ti interlayer becomes stronger with nitrogen gas and can provide increased support for the TiN coating, resulting in increased adhesion strength.

The result of the XRD analysis establishes the coating of Ti/TiN on the Ti-51 at% Ni sample at different DC power rate, as shown in Figure 4. The TiN-coated sample shows strong crystalline peaks which are detected at about 36.3°, 42.7°, 61.6°, 73.7°, and 77.32° corresponding to (111), (200), (220), (311) and (222) crystal planes of face centered cubic lattice respectively, having only TiN peaks present in the coating with space group 225: Fm-3m [29] which are consistent with file no ICDD 03-065-5759. These results are remarkably similar to TiN coatings deposited using magnetron sputtering and other PVD methods by other researchers [30-34]. The (111) orientation of TiN films is usually associated with the lowest strain energy, (200)

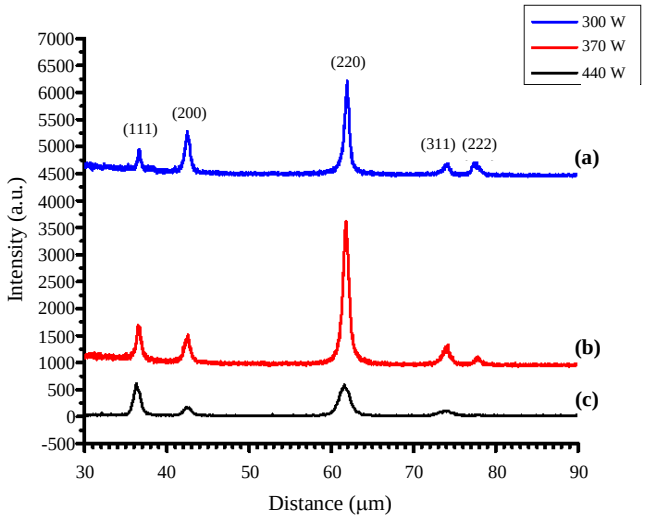

Figure 4. XRD spectrum of TiN coated on Ti-51 at% Ni at (a) 300 W, (b) 370 W, and (c) 440 W.

orientation is attributed to the lowest surface energy, and (220) occurs due to the lowest stopping energy which becomes dominant only when the deposited ion energy is high enough for the (220) peak to be observed [35]. As shown in Figure 4, (220) is the dominant preferred orientation observed, which indicates that the ion energy is sufficiently high at the DC power of 370 W and weak at 440 W. As DC power increased from 300 W to 370 W, as shown in Figures 4(a) and (b), peak intensities (111), (200) and (311) increased, while peak intensities (200) and (222) decreased. Meanwhile, the decrease in all the peaks and total disappearance of peak (222) was noticed in 4(c). The decrease in the film's crystallinity at 440W could be attributed to high-power sputtering that may likely cause a decrease in deposition rate and consequently causing low peaks formation. The preferred crystalline structure and orientation were further studied using the texture coefficient (TC) expression [36] :

$$TC(hkl) = \frac{I(hkl)/I_0(hkl)}{\frac{1}{N}\sum I(hkl)/I_0(hkl)} \quad (2)$$

Where TC (hkl) represent the texture coefficient for a particular reflection, I(hkl) is the peak intensities from the samples, I_0(hkl) is the intensity of a plane (hkl) referenced in ICDD card 03-065-5759, and N is the number of diffraction peaks that are taken into account when calculating the results.

The Texture coefficients calculated for (111), (200), (220), (311), and (222) planes at various DC power and film thickness are detailed in Table 2. The results show that maximum preferred orientation of the films along the (220) diffraction plane is indicated by the high value of TC along (220) planes at 370 W and 2.389 μm in thickness. This implies that the increased number of grains along that plane is related to the increase in preferred orientation. The TC is also seen to be influenced along (111) crystal orientation by the change in the film density and DC power. The higher the texture coefficient, the more preferred orientation of the films along that diffraction plane.

3.2 Effect of power on the thickness of Ti/TiN coating

The Ti-51 at% Ni, coated with T/TiN under different power rate, as shown in Figure 5 indicated that deposition at 370 W gave the highest thickness while at 440 W had the lowest thickness. It was observed that with the increase in DC power from 300 W to 370 W, the thickness also increased from 2.278 μm to 2.389 μm. However, when the DC power was increased to 440 W, the coating thickness decreased to 2.066 μm. The decrease in thickness could be attributed to a sharp drop in the sputtering rate due to high-power sputtering.

3.3 Microhardness test

The hardness test results on uncoated and coated Ti-51 at% Ni using microhardness tester (SHIMADZU Micro Hardness Tester, HMV-2 Series) showed that the hardness of the substrate increased with increase in DC power from 300 W to 370 W and decreased relatively with further increase in DC power to 440 W. The lower density of the thin film at 300 W and lower texture coefficient at the low strain energy plane could explain the coating's higher hardness

Table 2. Texture coefficient calculated for TiN film at various DC power, thickness and density.

DC Power	No.	h	k	l	d-spacing (Å)	2Theta (deg)	Height (count)	Size (Å)	TC (hkl)	I (%)	Thickness (μm)	Density (g·cm^{-3})
300 W	1	1	1	1	2.453	36.61	240	213	0.116	12		
	2	2	0	0	2.124	42.53	443	117	0.216	22		
	3	2	2	0	1.498	61.90	1125	154	0.548	55	2.278	4.37
	4	3	1	1	1.279	74.00	117	125	0.059	6		
	5	2	2	2	1.233	77.31	125	106	0.061	6		
370 W	1	1	1	1	2.458	36.52	407	131	0.155	16		
	2	2	0	0	2.125	42.50	275	96	0.105	11		
	3	2	2	0	1.501	61.73	1758	116	0.669	67	2.389	5.35
	4	3	1	1	1.281	73.90	181	92	0.069	7		
	5	2	2	2	------	------	------	------	------			
440 W	1	1	1	1	2.455	36.56	328	164	0.303	30		
	2	2	0	0	2.123	42.54	219	87	0.201	20		
	3	2	2	0	1.500	61.78	472	111	0.431	43	2.066	5.36
	4	3	1	1	1.280	73.98	74	90	0.066	7		
	5	2	2	2	------	------	------	------	------			

at 400 W when compared to deposition at 300 W. The optical micrograph showing the area influenced by the micro indentation and hardness value of Ti-51 at% Ni before coating and after coating are shown in Figure 6 (a) and (b). The increment in surface hardness after coating showed that deposition at DC power 370 W increased by 53.42%, indicating the highest hardness. Table 3 shows the average hardness computation and their percentage increment.

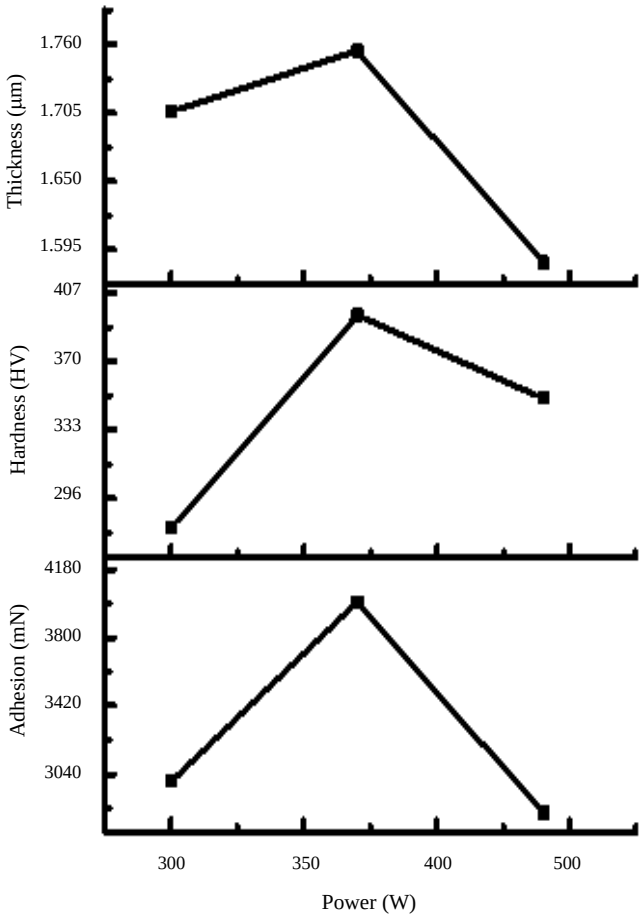

Figure 5. The effect of power on: (a) Thickness, (b) Hardness and (c) Adhesion.

3.4 Scratch adhesion Test

Scratch test was performed on TiN-coated Ti-51 at% Ni sample to determine the adhesion strength at 300 W, 370 W and 440 W DC power. The amount of adhesion strength between Ti-51 at% Ni and TiN was determined by the total coating failure (Lc2). Figure 7 displays the scratch track and the residual scratch track profiles in terms of load and depth with regards to scan distance. The line drawn indicates the sudden graph change that matches the coating failure startup. The critical loads in which the failures occur depend not only on the strength of the coating adhesion but also on other parameters, such as the traverse speed, the rate of increases in normal force and diamond-tip wear linked to the scratch test itself [37].

During the scratch test, the scratch length was 1,000 μm and 3000 mN to 4000 mN load with a loading rate of 3 $mN{\cdot}s^{-1}$. The test result shows adhesive failure at the distance of 946.66 um, 807.64 um and 852.76 um with critical load (Lc2) of 3000 mN, 3998 mN and 2825 mN respectively as shown in Table 4; this indicates that the deposition conducted at 370 W gave the highest adhesion strength. As power increased from 3000 W to 370 W, adhesion strength increased from 3000 mN to 3998 mN and decreased to 2825 mN when the power was increased to 440 W. The decreasing trend in the values of properties observed in thickness and hardness measurements could be linked to other parameters that are deliberately kept constant to observe only the effect of DC power. Increasing the DC power under constant pressure, increases the ion concentration in the chamber. The rate of sputtering rate increases as more power is applied. When power is increased further, it reduces the sputtering due to back-diffusion. As the power increased to 300 W and 370 W, more energy was gained by the electrically charged ionised and sputtered particles, which increased the sputtering rate and improved the thickness, adhesion strength and surface hardness. Alternatively, when the power increases further to 440 W, an increase in the collision between chamber particles and sputtered particles was observed. Consequently, there is a significant drop in the sputtering rate due to high power sputtering, which eventually led to a decrease in thickness, adhesion strength and surface hardness.

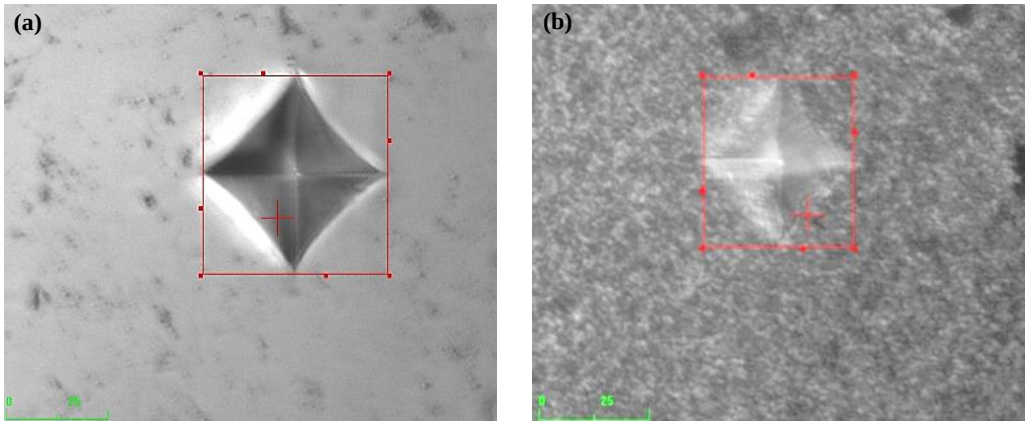

Figure 6. Optical micrograph showing the area influenced by the micro indentation and hardness value of Ti-51 at% Ni (a) before coating, and (b) after coating.

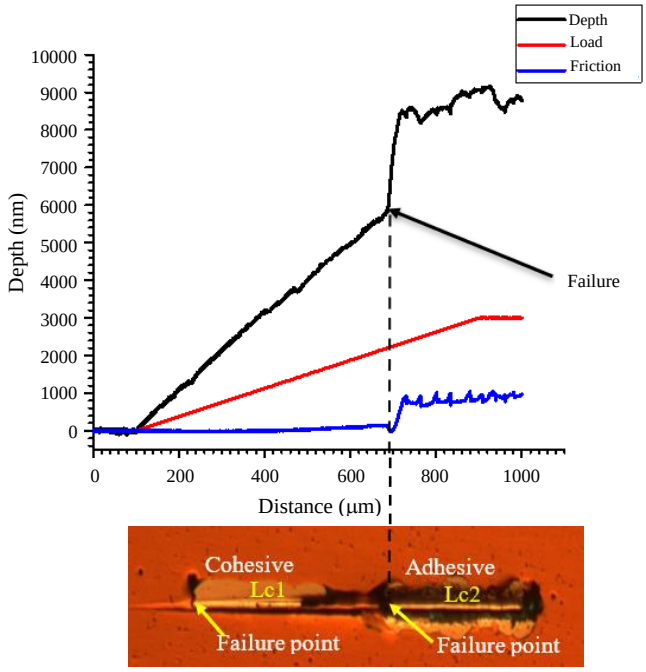

Figure 7. A graph of depth versus distance is compared with a scratch track micrograph.

Table 3. Average hardness computation.

Parameters	Uncoated	Coated		
Power (W)		300	370	440
First reading	132	301	438	344
Second reading	199	294	379	350
Third reading	222	265	367	334
Average hardness (HV)	184	287	395	343
Increase in hardness (%)		35.89	53.42	46.36

Table 4. Scratch adhesion strength test results.

Power (W)	Load (mN)	Distance (μm)
300	3000	946.66
370	3998	807.64
440	2825	852.76

4. Conclusions

The uncoated Ti-51 at% Ni alloy was characterised in this work by using optical microscopy(OM), SEM/EDX. DC magnetron sputtering technique was used to deposit Ti/TiN on Ti-51 at% Ni by varying 300 W, 370 W, and 440 W DC power. The effects of the varied parameters on the thickness, surface hardness and adhesion strength were studied through FESEM/EDX, XRD, microhardness and scratch testing. The following conclusion was deduced from the coating process:

- The optical microscopic observation results show that the Ti-51 at% Ni alloy has an equiaxed microstructure with well-distributed grain size and SEM/EDX micrograph shows the surface topography and elemental composition of the alloy.
- XRD analysis shows that, as the power increased from 300 W to 370 W, the peak intensities (111), (200), and (311) increased, while the reduction in peaks (200) and (222) was noticed. Meanwhile, the decrease in all the peaks and total disappearance of peak (222) at 440 W was noticed.
- The decrease in the film's crystallinity at 440 W could be attributed to high-power sputtering that may likely cause a decrease in deposition rate and consequently causing low peaks formation.
- As the power increased from 300 W to 370 W, the thickness also increased from 2.278 μm to 2.389 μm. However, when the power was increased to 440 W, the coating thickness decreased to 2.066 μm. The decrease in thickness may be caused by a sharp drop in the sputtering rate due to high-power sputtering.
- The substrate's hardness increased with increased power from 300 W to 370 W and decreased relatively, with further increase in power to 440 W. The increase in surface hardness after coating showed that deposition at power 370 W increased by 53.42%, indicating the highest hardness.
- It is noted that with the increase in DC power from 3000 W to 370 W, the adhesion strength increased from 3000 mN to 3998 mN and decreased to 2825 with further increase in DC power to 440 W.

Acknowledgements

The authors wish to thank the management of Universiti Teknologi Malaysia (UTM) for providing the financial support under Research University Grant (No. Q.J130000.2524.18H99) and Department of Mechanical Engineering University of Malaya (UM) for the research facilities

References

[1] Y. Ji, D. Wang, X. Ding, K. Otsuka, and X. Ren, "Origin of an isothermal R-martensite formation in Ni-rich Ti-Ni solid solution: crystallization of strain glass," *Physical Review Letters*, vol. 114, no. 5, pp. 055701, 2015.

[2] R. Pfeifer, C. W. Müller, C. Hurschler, S. Kaierle, V. Wesling, and H. Haferkamp, "Adaptable orthopedic shape memory implants," *Procedia CIRP*, vol. 5, pp. 253-258, 2013.

[3] M. Niinomi, M. Nakai, and J. Hieda, "Development of new metallic alloys for biomedical applications," *Acta Biomaterialia*, vol. 8, no. 11, pp. 3888-3903, 2012

[4] K. Yamauchi, I. Ohkata, K. Tsuchiya, and S. Miyazaki, eds, "Shape memory and superelastic alloys," *Applications and technologies*, Elsevier, 2011.

[5] J. Y. Xiong, Y. C. Li, P. D. Hodgson, and C. E. Wen, "Design of a new biocompatible Ti-based shape memory alloy and its superelastic deformation behaviour," *Materials Science Forum*, vol. 654, pp. 2087-2090, 2010.

[6] Y. Zhang, Z. W. Zhang, Y. M. Xie, S. S. Wang, Q. H. Qiu, Y. L. Zhou, and G. H. Zeng, "Toxicity of nickel ions and comprehensive analysis of nickel ion-associated gene expression profiles in THP-1 cell," *Molecular Medicine Reports*, vol. 12, no. 3, pp. 3273-3278, 2015

[7] S. A. Bernard, V. K. Balla, N. M. Davies, S. Bose, and A. Bandyopadhyay, "Bone cell–materials interactions and Ni ion release of anodized equiatomic NiTi alloy," *Acta Biomaterialia*, vol. 7, no. 4, pp. 1902-1912, 2011.

[8] M. Brojan, D. Bombač, F. Kosel, and T. Videnič, "Shape memory alloys in medicine," *RMZ-Mater and Geoenvir*, vol 55, no. 2, pp. 173-189, 2008.

[9] B. Subramanian, R. Ananthakumar, and M. Jayachandran, "Structural and tribological properties of DC reactive magnetron sputtered titanium/titanium nitride (Ti/Tin) multi-layered coatings," *Surface and Coating Technology*, vol. 205, no. 11, pp. 3485-3492, 2011

[10] Y. Luo, and S. Ge, "Fretting wear behaviour of nitrogen ion implanted titanium alloys in bovine serum lubrication," *Tribology International*, vol. 42, no. 9, pp. 1373-1379, 2009.

[11] R. Polini, M. Barletta, and G. Cristofanilli, "wear resistance of nano- and micro-crystalline diamond coatings onto WC-Co with Cr/CrN interlayers," *Thin Solid Films*, vol. 519, no. 5, pp. 1629-1635, 2010.

[12] G. Cassar, J. A. B. Wilson, S. Banfield, J. Housden, A. Matthews, and A. Leylan, "A study of the reciprocating-sliding wear performance of plasma surface treated titanium alloy," *Wear*, vol. 269, no. 1-2, pp. 60-70, 2010.

[13] S. Sathish, M. Geetha, S. T. Aruna, N. Balaji, K. S. Rajam, and R. Asokamani, "Sliding wear behaviour of plasma sprayed nanoceramic coatings applications," *Wear*, vol. 271, pp. 934-941, 2011.

[14] S. Shabalovskaya, J. Anderegg, and J. Van Humbeeck, "Critical overview of Nitinol surfaces and their modifications for medical applications," *Acta Biomaterialia*, vol. 4, no. 3, pp. 447-467, 2008.

[15] M. F. Maitz, (2009) "Surface modification of Ti–Ni alloys for biomedical applications. In Shape Memory Alloys for Biomedical Applications," in *Shape Memory Alloys for Biomedical Applications*, Woodhead Publishing, 2009, pp. 173-193,

[16] M. F. Othman, A. R. Bushroa, and W. N. R. Abdullah. "Evaluation techniques and improvements of adhesion strength for TiN coating in tool applications: a review *Journal of Adhesion Science and Technology*, vol. 29, no. 7, pp. 569-591, 2015

[17] Y. Yang, K. H. Kim, and J. L. Ong, "A review on calcium phosphate coatings produced using a sputtering process—an alternative to plasma spraying," *Biomaterials*, vol. 26, no. 3, pp. 327-337, 2005.

[18] A. Shah, S. Izman, and S. N. Fasehah, "Study on micro droplet reduction on TiN coated biomedical Ti-13Zr-13Nb alloy," *Jurnal Teknologi*, vol. 78, pp. 5-10, 2016.

[19] A. Shah, S. Izman, and M. A. Hassan, "Influence of nitrogen flow rate in reducing tin microdroplets on biomedical Ti-13Zr-13Nb alloy," *Jurnal Teknologi*, vol. 78, pp. 6-10, 2016.

[20] Y. H. Yang, D. J. Chen, and F. B. Wu, "Microstructure, hardness, and wear resistance of sputtering TaN coating by controlling RF input power," *Surface Coating Technology*, vol. 303, pp. 32-40, 2016

[21] S. Piscanec, L. C. Ciacchi, E. Vesselli, G. Comelli, O. Sbaizero, S. Meriani, and A. De Vita, "Bioactivity of TiN-coated titanium implants," *Acta Materials*, vol. 52, no. 5, pp. 1237-1245, 2004.

[22] R. W. Poon, J. P. Ho, X. Liu, C. Chung, P. K. Chu, K. W. Yeung, W. W. Lu, K. M. Cheung, "Formation of titanium nitride barrier layer in nickel–titanium shape memory alloys by nitrogen plasma immersion ion implantation for better corrosion resistance," *Thin Solid Films*, vol. 488 no. 1, pp. 20-25, 2005.

[23] K. Yeung, R. Poon, X. Liu, J. Ho, C. Chung, P. Chu, W. Lu, D. Chan, and K. Cheung, "Corrosion resistance, surface mechanical properties, and cytocompatibility of plasma immersion ion implantation–treated nickel-titanium shape memory alloys," *Journal of Biomedical Materials Research Part A*, vol. 75, no. 2, pp. 256-267, 2005,

[24] D. Starosvetsky, and I. Gotman, "Corrosion behaviour of titanium nitride coated Ni–Ti shape memory surgical alloy" *Biomaterials*, vol. 22, 13, pp. 1853-1859, 2001.

[25] B. D. Beake, V. M. Vishnyakov, R. Valizadeh, and J. S. Colligon, "Influence of mechanical properties on the nanoscratch behaviour of hard nanocomposite TiN/Si3N4 coatings on Si," *Journal of Physics D: Applied Physics*, vol. 39, no. 7, pp. 1392, 2006.

[26] A. Shah, S. Izman, S. N. F. Ismail, H. Mas-Ayu, and R. Daud, "Study on adhesion strength of TiN coated biomedical Ti-13Zr-13Nb alloy," *Journals Teknologi*, vol. 80, no. 2, 2018.

[27] A. Mubarak, and E. Hamzah, "Influence of Nitrogen Gas Flow Rate on The Microstructural and Mechanical Properties of Tin Deposited Carbon Steel Synthesized by Cae," *ASEAN Journal on Science and Technology for Development*, vol. 22, no 4, pp. 239-251, 2006.

[28] Y. ChunyanT. Linhai, W. Yinghui, W. Shebin, L. Tianbao, and X. Bingshe, "The effect of substrate bias voltages on impact resistance of CrAlN coatings deposited by modified ion beam enhanced magnetron sputtering," *Applied Surface Science*. vol. 255, no. 7, pp. 4033-4038, 2009.

[29] A. R. Bushroa, H. H. Masjuki, M. R. Muhamad, "Parameter optimization of sputtered Ti interlayer using Taguchi method," *International Journal of Mechanical and Materials Engineering*, vol. 6, no. 2, pp. 140-146, 2011.

[30] B. Subramanian, C. V. Muraleedharan, R. Ananthakumar, and M. Jayachandran, "A comparative study of titanium nitride (TiN), titanium oxy nitride (TiON) and titanium aluminum nitride (TiAlN), as surface coatings for bio-implants," *Surface Coating Technology*, vol. 205, no. 21-22, pp. 5014-5020, 2011.

[31] Y. Fu, H. Du, and S. Zhang, "Deposition of TiN layer on TiNi thin films to improve surface properties," *Surface Coating Technology*, vol. 167, no. 2-3, pp. 129-136, 2003

[32] A. Y. Chen, Y. Bu, Y. T. Tang, Y. Wang, F. Liu, X. F. Xie, and J. F. Gu, "Deposition-rate dependence of orientation growth and crystallization of Ti thin films prepared by magnetron sputtering," *Thin Solid Films*, vol. 574, pp. 71-77, 2015.

[33] S. Jin, Y. Zhang, Q. Wang, D. Zhang and S. Zhang, "Influence of TiN coating on the biocompatibility of medical NiTi alloy," *Colloids and Surfaces B: Biointerfaces*, vol. 101, pp. 343-349, 2013.

[34] F. Vaz, L. Rebouta, P. Goudeau, T. Girardeau, J. Pacaud, J. P. Riviere, and A. Traverse, "Structural transitions in hard Si-based TiN coatings: the effect of bias voltage and temperature," *Surface Coating Technology*, vol. 146, pp. 274-279, 2001.

[35] C. Zhang, T. Hu, and N. Zhang, "Influence of substrate hardness on coating-substrate adhesion," in *Advanced Materials Research*, vol. 177, pp. 148-150. Trans Tech Publications Ltd, 2011.

[36] Y. Wang, W. Tang, and L. Zhang. "Crystalline size effects on texture coefficient, electrical and optical properties of sputter-deposited Ga-doped ZnO thin films." *Journal of Materials Science & Technology*, vol. 31, no. 2, pp. 175-181, 2015.

[37] T. Jiang, N. Hall, A. Ho, and S. Morin, “Quantitative analysis of electrodeposited TiN film morphologies by atomic force microscopy,” *Thin Solid Films*, vol. 471, no. 1-2, pp. 76-85, 2005.